The Journal of Immunology

The Effect of Adjuvanting Cancer Vaccines with Herpes Simplex Virus Glycoprotein D on Melanoma-Driven CD8$^+$ T Cell Exhaustion

Ying Zhang and Hildegund C. J. Ertl

J Immunol 2014; 193:1836-1846; Prepublished online 14 July 2014;
doi: 10.4049/jimmunol.1302029
http://www.jimmunol.org/content/193/4/1836

The Journal of Immunology is published twice each month by
The American Association of Immunologists, Inc.,
1451 Rockville Pike, Suite 650, Rockville, MD 20852

Print ISSN: 0022-1767 Online ISSN: 1550-6606.

The Effect of Adjuvanting Cancer Vaccines with Herpes Simplex Virus Glycoprotein D on Melanoma-Driven CD8$^+$ T Cell Exhaustion

Ying Zhang* and Hildegund C. J. Ertl*,†

Two vaccines expressing CD4$^+$ and CD8$^+$ T cell epitopes of melanoma-associated Ags (MAAs) by a chimpanzee-derived replication-defective AdC68 vector were compared in a mouse model of melanoma. In one vaccine, termed AdC68-gDMelapoly, the epitopes were expressed as a fusion protein within HSV-1 glycoprotein D (gD), which blocks immunoinhibitory signaling through the herpes virus entry mediator pathway. The other vaccine, termed AdC68-Melapoly, expressed only the MAA epitopes. AdC68-gDMelapoly induced more potent MAA-specific CD8$^+$ T cell responses especially to the subdominant MAA epitopes. Upon prophylactic vaccination, mice that developed CD8$^+$ T cell responses to the two vaccines that were comparable in magnitude showed equal protection against tumor challenge. When mice were first challenged with tumor cells and then vaccinated results differed. In animals with comparable CD8$^+$ T cell responses, the AdC68-gDMelapoly vaccine was more efficacious compared with the AdC68-Melapoly vaccine in delaying tumor growth. This effect was linked to reduced expression of 2B4, LAG-3, and programmed death-1 on tumor-infiltrating MAA-specific CD8$^+$ T cells elicited by the gD-adjuvanted vaccine, suggesting that CD8$^+$ T cells induced in presence of gD are less susceptible to tumor-driven exhaustion. ***The Journal of Immunology*****, 2014, 193: 1836–1846.**

Even cancer vaccines that are highly immunogenic in animal models commonly fail to provide benefits to patients with advanced cancers (1, 2). This has partially been linked to the highly immunosuppressive tumor microenvironment, which expresses immunoinhibitory ligands (3), recruits suppressive cell subsets such as regulatory T cells (4) and myeloid suppressor cells (5) and provides a metabolically stressed milieu (6). Biologicals that block immunoinhibitory pathways such as Abs to programmed death-1 (PD-1) (7, 8) or CTLA-4 (9) or both (10, 11) are being tested alone or in combination with active immunotherapy in cancer patients and have yielded promising results.

Our focus has been on the herpes virus entry mediator (HVEM) pathway. HVEM, which was first identified as a receptor for HSV-1 glycoprotein D (gD) (12), is a bimodal switch expressed on many cells including Ag presenting cells that can interact with the immunoregulatory molecules on lymphocytes (13). Binding of HVEM to LIGHT or lymphotoxin provides stimulatory signals; binding to the B and T lymphocyte attenuator (BTLA) or CD160 activates inhibitory pathways (14). Coactivators and coinhibitors bind to different domains of HVEM and can form a trimolar complex, in which signaling through coinhibitors dominates (14). The N-terminus of HSV-1 gD binds to a site on HVEM that is close to the BTLA/CD160 binding site and thereby blocks immunoinhibitory but not costimulatory HVEM signaling (15).

As we have shown previously, vaccines that express Ags fused into the C terminus of gD elicit enhanced T cell responses, which is linked to blockade of the immunoinhibitory HVEM pathways (16). Adjuvanting vaccine Ags with gD is especially effective to augment CD8$^+$ T cell responses in aging mice (17) and in mice with advanced cancers (18). Our previous cancer studies were based on human papilloma virus type 16–associated tumors, which express viral Ags that are foreign to the immune system. The current study was conducted to assess whether expressing "self'' Ags from nonviral tumors within gD would enhance the immunogenicity and efficacy of a cancer vaccine. Experiments were conducted in a transplantable melanoma model, based on B16F10 cells that were stably transfected to express $Braf_{V600E}$ ($B16Braf_{V600E}$). The vaccine Ag, termed Melapoly, was designed to express CD4$^+$ and CD8$^+$ T cell epitopes of melanoma-associated Ags (MAAs) including tyrosinase-related protein (Trp)-1, Trp-2, gp100 and mutated $Braf_{V600E}$ linked to the universal Th cell epitope PADRE and an endoplasmic reticulum targeting signal sequence. To test for the gD adjuvant effect, the Melapoly encoding sequence was fused into the C terminal domain of HSV-1 gD (gDMelapoly). The Melapoly and the gDMelapoly fusion proteins were expressed by a simian E1-deleted adenovirus vector of serotype 68 (AdC68).

As expected, the AdC68-gDMelapoly vector induced more potent MAA-specific CD8$^+$ T cell responses, especially to subdominant epitopes, compared with the AdC68-Melapoly vector and provided superior protection if given before tumor challenge. In the same token, in a therapeutic vaccination model, the AdC68-gDMelapoly vector was superior in delaying tumor progression compared with the AdC68-Melapoly vector. To assess whether the improved efficacy of the gD-adjuvanted vaccine solely reflected differences in the magnitude of MAA-specific T cell responses, we vaccinated mice with different doses of the AdC68 vectors and selected subgroups with comparable frequencies of MAA-specific

*Gene Therapy and Vaccines Program, University of Pennsylvania School of Medicine, Philadelphia, PA 19104; and †Wistar Institute Vaccine Center, University of Pennsylvania, Philadelphia, PA 19104

Received for publication August 19, 2013. Accepted for publication June 7, 2014.

This work was supported by funds from the Wistar Institute Vaccine Center.

Address correspondence and reprint requests to Dr. Hildegund C.J. Ertl, Wistar Institute Vaccine Center, 3601 Spruce Street, Philadelphia, PA 19104. E-mail address: ertl@wistar.upenn.edu

The online version of this article contains supplemental material.

Abbreviations used in this article: AdC68, adenovirus vector of serotype 68; BTLA, B and T lymphocyte attenuator; gD, glycoprotein D; HVEM, herpes virus entry mediator; ICS, intracellular cytokine staining; MAA, melanoma-associated Ag; MFI, mean fluorescence intensity; PD-1, programmed death-1; TIL, tumor-infiltrating lymphocyte; Trp, tyrosinase-related protein; vp, virus particle.

www.jimmunol.org/cgi/doi/10.4049/jimmunol.1302029

$CD8^+$ T cells. In a prechallenge vaccination model, vaccine efficacy was shown to depend on frequencies of MAA-specific $CD8^+$ T cells. In contrast in a postchallenge vaccination model, AdC68-gDMelapoly–vaccinated mice that had MAA-specific T cell frequencies comparable to those of AdC68-Melapoly–vaccinated mice survived significantly longer. This was not caused by differences in production of mediators by AdC68-gDMelapoly-induced T cells but rather by their increased resistance against differentiation toward exhaustion.

Materials and Methods

Mice

Female C57BL/6 mice (6–8 wk) were purchased from the National Cancer Institute and housed at the Wistar Institute Animal Facility. All procedures were performed under the guideline of protocols approved by the Institutional Animal Care and Use Committee of the Wistar Institute.

Cell lines

The $B16Braf_{V600E}$ cell line was derived from B16.F10 cells transduced with lentiviral vector pLU-EF1a-mCherry expressing mouse $Braf_{V600E}$ (provided by Dr. M Herlyn laboratory, Wistar Institute). The mutant cell line showed the same in vivo growth characteristics as unmodified B16.F10 cells. E1-transfected HEK 293 cells were used to propagate Ad vectors. Cells were cultured with DMEM supplemented with 10% FBS.

Construction of recombinant Ad vectors

We designed the Melapoly transgene to express a number of MAA-specific $CD4^+$ T cell and $CD8^+$ T cell epitopes. An endoplasmic reticulum targeting signal sequence was included at the N-terminal end of the sequence (19). Three human (h)Trp-2-specific $CD4^+$ T cell epitopes (20) as well as the universal Th cell epitope PADRE (21) were incorporated into the Melapoly construct. $CD8^+$ T cell epitopes were derived from human and mouse Trp-2, human gp100, mouse Trp-1, and $Braf_{V600E}$. Epitopes from Trp-1 and Braf Ags were modified to enhance their binding to MHC class I molecules (22). A Flag-tag was added to the C-terminal end. We designed the spacer sequences according to several analysis programs, including PAPROC I (http://www.paproc.de), Netchop 3.1 (http://www.cbs.dtu.dk/services/NetChop/), and IEBD Analysis Resource (http://tools.immuneepitope.org/main/). The spacers were inserted between each $CD4^+$ and $CD8^+$ T cell epitope to reduce interference of epitope processing (23, 24). The Melapoly gene was codon optimized and inserted into the pUC57 vector (Genescript, Piscataway, NJ). The Melapoly transgene was sequenced and cloned it into the pShuttle vector by EagI digestion. To construct the AdC68-gDMelapoly vector, the Melapoly transgene was fused into the N terminus of HSV-1 gD. The pShuttle gDMelapoly vector was generated by PCR using pShuttle Melapoly as the template, gDMelaFwAgeI 5′-CGACCGGTTAGCTAAGTTTGTGGCCGCTTG-3′ and gDMelaRvAvrII 5′-CGCCTAGGTGCTGCTGCTGCAATGCTC-3′ as primers. The PCR product was cleaved by AgeI and AvrII and cloned into the pShuttle gD-Flag vector. The inserts containing regulatory sequences of the pShuttle vector were subcloned into the E1-deleted AdC68 viral molecular clone using I-CeuI and PI-SceI sites. Recombinant AdC68 vectors were rescued, propagated on HEK 293 cells, purified by CsCl-gradient centrifugation and titrated as described previously (25). The concentration of each virus batch was determined by measuring virus particles (vp) by spectrophotometry at 260 nm.

Real-time PCR

We infected HEK 293 cells with 10^{10} and 10^{11} vp doses of AdC68-Melapoly and AdC68-gDMelapoly vectors. Cells were harvested 24 h later and total RNA was isolated from each sample using RNeasy Mini Kit (Qiagen, Venlo, The Netherlands). cDNA samples were obtained by reverse transcription using 2 μg RNA/sample with high capacity cDNA reverse transcription kit (Applied Biosystems, Foster City, CA). Twenty nanograms of cDNA per sample was used for real-time PCR using Fast SYBR green Mastermix (Applied Biosystems). To obtain standards for real-time PCR, we performed regular PCR for Melapoly and GAPDH (housekeeping gene as internal control) using the cDNA samples. We ran the PCR products on 1% agarose gel, purified the PCR products of the expected sizes (MiniElute gel extraction kit; Qiagen) and measured the DNA concentration using spectrometry. We diluted the purified Melapoly and GAPDH DNAs from 5 to 0.156 ng for real-time PCR standards. For real-time PCR, cDNA samples were replicated for both Melapoly and GAPDH using the 7500 Fast Real-Time PCR machine (Applied Biosystems). The primer sequences are as follows: regular PCR MelapolyFw 5′-ACAGGAAACTTCGCCGCTGC, MelapolyRv 5′-TGCCATATATCCGAGGTTGTCTG-3′, real-time PCR MelapolyRv1 5′-TGATCGGCTGCAGCCACGTC-3′; regular PCR GAPDHFw 5′-GGGGTCGGTGTGAACGGATTT-3′, GAPDHRv 5′-AATGCCAAAGTTGTCATGGATGACC-3′ and real-time PCR GAPDHFw1 5′-TGCCCCCATGTTTGTGATGG-3′. The final concentrations of Melapoly cDNA from both vector-infected samples were analyzed and compared after normalization to GAPDH.

Immunization and challenge of mice

Groups of C57BL/6 mice were vaccinated i.m. with the AdC68 vectors diluted in PBS into the tribialis anterior muscle of each hind limb, with doses ranging from 3×10^9 to 10^{11} vp per mouse. In tumor challenge experiments, $B16Braf_{V600E}$ cells suspended in serum-free medium were inoculated s.c. into the right flank of mice. For pre- and posttumor challenge experiments, 5×10^4 cells were injected and mice were vaccinated 14 d before or 3 d after tumor cell challenge. We monitored tumor growth by measuring the perpendicular diameters of tumors at least three times a week. Mice were euthanized once tumors exceeded a surface area of 100 mm^2. Mice were monitored for a period of 60 d posttumor challenge.

Isolation of lymphocytes

PBMCs and splenocytes were harvested as described before (18). To obtain tumor-infiltrating lymphocytes (TILs), tumors were cut into small fragments and treated with 2 mg/ml collagenase P and 1 mg/ml DNase I (Life Technologies, Carlsbad, CA) diluted in Hank's balanced salt solution (1× HBSS) (Thermo Fisher Scientific, Pittsburgh, PA) with agitation for 1 h. Tumor fragments were homogenized and filtrated, and lymphocytes were purified by Percoll-gradient centrifugation.

Tetramer and intracellular cytokine staining

To detect tetramer-specific $CD8^+$ T cells, we stained cells with a PE-labeled Trp-1–specific MHC class I ($H\text{-}2D^b$) tetramer carrying the TAPDNLGYM peptide and an Alexa647–labeled tyrosinase-related protein 2 MHC class I ($H\text{-}2K^b$) tetramer carrying the SVYDFFVWL peptide (obtained from the National Institute of Allergy and Infectious Diseases Tetramer Facility, Atlanta, GA). The following Abs were also used for staining: anti–CD8-PerCPCy5.5, PacBlue or Alexa700, CD4-PercpCy5.5, CD44-PacBlue or Alexa700, LAG-3 PercpCy5.5, PD-1 PE-Cy7 (all from BioLegend, San Diego, CA), 2B4 FITC (eBioscience, San Diego, CA), and Amcyan fluorescent reactive dye (Life Technologies). For intracellular cytokine staining (ICS), $CD8^+$ and $CD4^+$ T cell responses to individual epitopes were measured using $\sim 10^6$ lymphocytes/samples. Cells were cultured in 2% FBS DMEM with individual MHC class I or class II–restricted peptides at a concentration of 5 μg/ml (for peptides representing $CD8^+$ T cell epitopes): $mTrp\text{-}1_{455–463}$ TAPDNLGYA, $mTrp\text{-}1_{481–489}$ IAVVAALLL, $mTrp\text{-}2_{522–529}$ YAEDYEEL, $hTp\text{-}2_{180–188}$ SVYDFFVWL, $hTrp\text{-}2_{343–357}$ STFSFRNAL, $mTrp\text{-}2_{363–371}$ SQVMNLHNL, $hgp100_{25–33}$ KVPRNQDWL, and $mBRaf_{594–602}$ FGLANEKSI; or 10 μg/ml (for peptides representing $CD4^+$ T cell epitopes): PADRE: AKFVAAWTLKAAA, $hTrp\text{-}2_{88–102}$: RKFFHRTCKCTGNFA, $hTrp\text{-}2_{237–256}$: NESFALPYWNFATGRNECDV and $mTrp\text{-}2_{363–376}$: SQVMNLHNLAHSPL (Genescript, Piscataway, NJ). To determine overall MAA-specific T cell responses, a peptide pool including all $CD8^+$ and $CD4^+$ T cell epitopes expressed by the Melapoly or gDMelapoly vectors was used for lymphocytes stimulation. A rabies virus glycoprotein peptide was used as a negative control. ICS was conducted as described previously (14). Produced cytokines, enzymes were stained with the following Abs: anti–IFN-γ-allophycocyanin, IL-2-Alexa700 or FITC, and TNF-α-PE-Cy7 (BioLegend, San Diego CA). Transcription factor T-bet was stained using Foxp3/Transcription factor staining buffer set (eBioscience) using anti–T-bet-PE-Cy7 Ab (eBioscience). Cells tested by ICS were costained for exhaustion marker PD-1 using anti–PD-1-Brilliant Violet 605 Ab (BioLegend, San Diego CA). Cells were analyzed by an LSRII (BD Biosciences, Franklin Lakes, NJ). Data were analyzed with FlowJo (Tree Star, Ashland, OR). Experiments using ICS or tetramer stains were controlled assessing responses of $CD44^-CD8^+$ cells within the same animals after preliminary experiments confirmed that results were comparable to those obtained with $CD44^+$ $CD8^+$ cells of naive mice or mice vaccinated with the AdC68-gD control vector.

Statistical analysis

We compared the differences of immune responses between more than two groups using one-way ANOVA followed by Holm–Sidak's multiple comparisons. Immune responses affected by two factors (vaccine and

tissue type or vaccine and cell type) were analyzed by two-way ANOVA with Holm-Sidak's multiple comparisons. We performed Holm–Bonferroni correction for multiple comparisons within the same dataset. Survival rates between different treatment groups were compared using Gehan-–Breslow–Wilcoxon test. Significance was set at $p \leq 0.05$. All statistical analyses were performed using Graphpad Prism6. Throughout the paper, p values adjusted for type 1 errors are shown.

Results

The gD adjuvant enhances CD8$^+$ T cell responses to dominant and subdominant epitopes

Levels of transgene expression can affect the immunogenicity of viral vectors. We therefore tested the levels of transgene product expression in transfected cells and showed by real-time PCR that both vectors expressed comparable levels of transgene-derived mRNA (data not shown).

We compared the magnitude of MAA-specific CD8$^+$ T cell responses induced by the vaccines in young female C57BL/6 mice. Each group (n = 5) of mice received either the AdC68-Melapoly or the AdC68-gDMelapoly vector given i.m. at doses of 10^{10} or 10^{11} vp. Two and four weeks after vaccination, we measured CD8$^+$ T cell responses to two MAA epitopes (i.e., Trp-1_{455} and Trp-2_{180}) by staining T cells with the corresponding MHC class I tetramers (Supplemental Fig. 1). Both vaccines induced stronger CD8$^+$ T cell responses to Trp-1_{455} than Trp-2_{180} (mean frequencies of positive CD44$^+$CD8$^+$ cells for Trp-1_{455} versus Trp-2_{180}: 10^{10} vp: week 2: Melapoly: 5.1 versus 0.56%, gDMelapoly: 5.8 versus 0.58%; week 4: Melapoly: 2.5 versus 0.25%, gDMelapoly: 5.3 versus 0.42%; 10^{11} vp: week 2: Melapoly: 8.7 versus 0.86%, gDMelapoly: 14.7 versus 0.51%; week 4: Melapoly: 7.8 versus 0.18%, gDMelapoly: 8.5 versus 0.56%; naive CD44$^-$ T cells: 0.043 versus 0.056 and 0.043 versus 0.078% for weeks 2 and 4, respectively, Fig. 1A, 1B). All groups mounted significant responses to the Trp-1_{455} and Trp-2_{180} tetramer compared with the internal CD44$^-$CD8$^+$ T cell controls (adjusted p values are listed in legend to Fig. 1) or to naive mice (data not shown). At the 10^{11} vp dose at week 2 and the 10^{10} vp dose at week 4 Trp-1_{455}–specific CD8$^+$ T cell responses were significantly higher in AdC68-gDMelapoly–vaccinated animals than in AdC68-Melapoly–vaccinated mice. Responses to Trp-2_{180} were significantly higher in mice vaccinated with 10^{11} vp AdC68-gDMelapoly at both weeks 2 and 4. At the 10^{10} vp dose at week 4 Trp-2_{180} responses were significantly higher in Melapoly-vaccinated mice.

To further assess differences, we immunized mice (n = 7–8) with 10^{11} vp of the AdC68-Melapoly vector or 10^{10} vp of the AdC68-gDMelapoly vector. We collected blood at different time points after vaccination and measured the immune responses to individual MAA epitopes by ICS for production of IFN-γ, TNF-α, and IL-2 (Fig. 2, Supplemental Fig. 2). For these experiments, blood had to be pooled to allow for testing the PBMC samples stimulated with the eight different peptides carrying CD8$^+$ T cell epitopes expressed by the vaccines. Both vectors induced significantly higher tumor-Ag–specific CD8$^+$ T cell responses to both dominant and subdominant epitopes compared with naive controls (CD44$^-$CD8$^+$ T cells). Despite the lower dose, there was a clear trend of the AdC68-gDMelapoly vaccine to induce higher responses mainly to the subdominant epitopes (Trp-1_{455} epitope: mean frequencies averaging all time points: 1.9 and 2.9% for Melapoly and gDMelapoly, respectively, Fig. 2A; subdominant epitopes: mean frequencies of the sum of responses averaging all time points 1.3 and 3.0% for Melapoly and gDMelapoly, respectively, Fig. 2B). The preferential increase of responses to subdominant epitopes by gD was confirmed by comparing responses to the dominant Trp-1_{455} epitope to those against the subdominant Trp-2_{180} epitope by tetramer staining at 4 and 26 wk after vaccination with 10^{11} vp AdC68-Melapoly or 10^{10} vp AdC68-gDMelapoly (Fig. 2C, 2D). At both early and late time points, the responses to Trp-1_{455} epitope were comparable, whereas the responses to Trp-2_{180} epitope were significantly higher in mice immunized with AdC68-gDMelapoly (week 4, mean tetramer frequencies for Trp-1_{455}: Melapoly versus gDMelapoly: 7.8 versus 5.3%; Trp-2_{180}: 0.18 versus 0.42%, p = 0.0053; week 26, Trp-1_{455}: Melapoly versus gDMelapoly: 4 versus 5.9%, Trp-2_{180}: 0.35 versus 0.66%, p = 0.033).

We selected three time points (weeks 6, 12, and 24) to compare the overall response pattern (Fig. 2E–J). Responses to the subdominant epitopes developed with a delay as compared with Trp-1_{455} responses. At all three time points the gD-adjuvanted vector induced a more prominent CD8$^+$ T cell response to the subdominant epitopes compared with the AdC68-Melapoly vector (sum of frequencies to Melapoly and gD-Melapoly, respectively: week 6: 3.8 and 4.4%; week 12, 2 and 6.7%; and week 24, 4.5 and 6.6%).

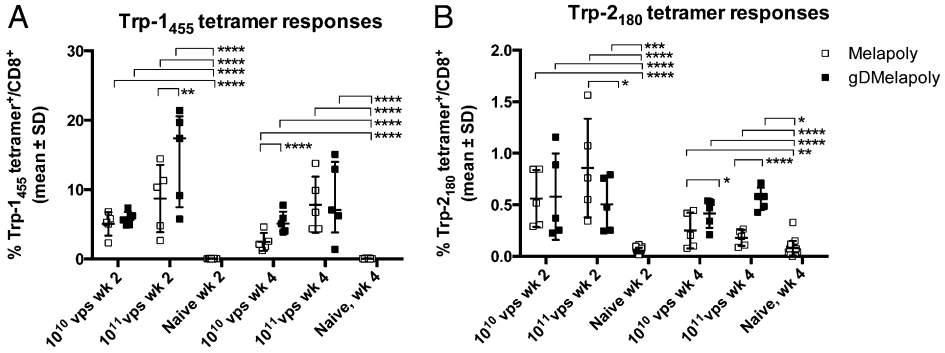

FIGURE 1. Induction of MAA-specific CD8$^+$ T cells by different vector doses. Groups (n = 5/group) of C57BL/6 mice were vaccinated i.m. with 10^{10} or 10^{11} vp of either AdC68-Melapoly (□) or AdC68-gDMelapoly (■) vector. PBMCs were collected 2 and 4 wk later, and (**A**) Trp-1_{455}- and (**B**) Trp-2_{180}-specific CD8$^+$ T cell responses were compared. The graphs show responses in individual animals, the lines indicate means ± SEs. *, Significant differences between groups connected by lines (*p = 0.01–0.05, ** p = 0.001–0.01, *** p = 0.0001–0.001, ****$p < 0.0001$). The following differences had significant p values: all groups Trp-1_{455} compared with CD44$^-$CD8$^+$ controls: $p < 0.0001$; Trp-1_{455}: Melapoly versus gDMelapoly: 10^{11} vp, wk 2: p = 0.012, 10^{10} vp, wk 4: $p < 0.0001$; Trp-2_{180} compared with controls: Melapoly, 10^{10} vp: wk 2: $p < 0.0001$, wk 4: p = 0.016; 10^{11} vp: wk 2: $p < 0.0001$, wk 4: p = 0.034; gDMelapoly: both doses and both time points: $p < 0.0001$; Trp-2_{180}: Melapoly versus gDMelapoly: 10^{11} vp: wk 2: p = 0.027, 10^{10} vp: wk 2: p = 0.036, wk 4: $p < 0.0001$.

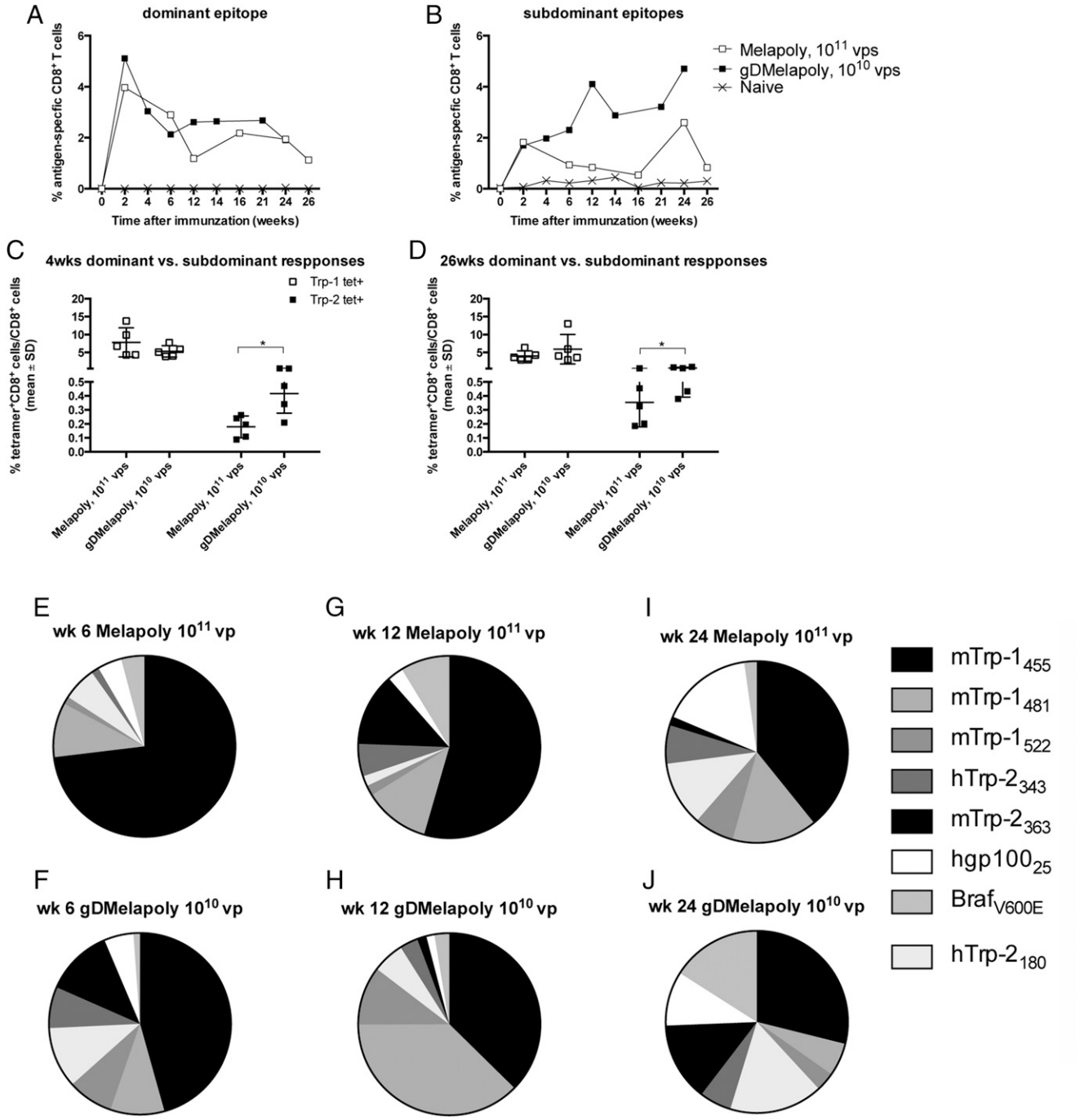

FIGURE 2. MAA-specific $CD8^+$ T cell responses to individual epitopes. Groups of C57BL/6 mice (n = 7–8) were vaccinated i.m. with 10^{11}vp AdC68-Melapoly or 10^{10}vp AdC68-gDMelapoly. (**A** and **B**) $CD8^+$ T cell responses to individual epitopes were measured by ICS for IFN-γ, TNF-α, and IL-2 upon stimulation of cells with peptides representing the T cell epitopes expressed by the vaccines over a course of 24–26 wk. Graphs show the sum of cytokine responses. (A) shows responses to the dominant Trp-1_{455} peptides. (B) shows the sum of responses over time for the other peptide; responses to individual peptides (but for Trp-1_{455}) were totaled. (**C**) and (**D**) shows Trp-1-teramer$^+$ and Trp-2 tetramer$^+$$CD8^+$ T cell responses 4 and 26 wk after vaccination in tumors of vaccinated mice. Differences between the two vaccines were not significant for Trp-1–specific $CD8^+$ T cells (p = 0.12 and 0.18, respectively) but significant for Trp-2–specific $CD8^+$ T cells (p = 0.0053 and 0.035, respectively). (**E**–**J**) The patterns of the sum of cytokine responses to the eight $CD8^+$ T cell epitopes at three time points [i.e., week 6 (E, F), 12 (G, H) and 24 (I, J)] after vaccination.

In a pretumor challenge vaccination model, gD adjuvant efficacy is solely linked to magnitude of the MAA-specific $CD8^+$ T cell responses

To determine whehter vaccination with the AdC68-gDMelapoly vector resulted in superior protection against tumor growth than vaccination with the AdC68-Melapoly vector, we immunized groups of mice (n = 5–18) with 10^{10} vp AdC68-gDMelapoly, 10^{11} vp AdC68-Melapoly or 10^{11} vp AdC68-gD, the latter as a control for nonspecific effects of the vector or gD. Fourteen days later, mice were challenged with $B16Braf_{V600E}$ cells given s.c. Total cytokine$^+$$CD8^+$ T cell responses to the eight $CD8^+$ T cell epitopes were measured before tumor challenge. As shown in Fig. 3A, both vaccines induced significantly higher responses when compared with background stains of naive T cells (mean frequencies 4.5 and

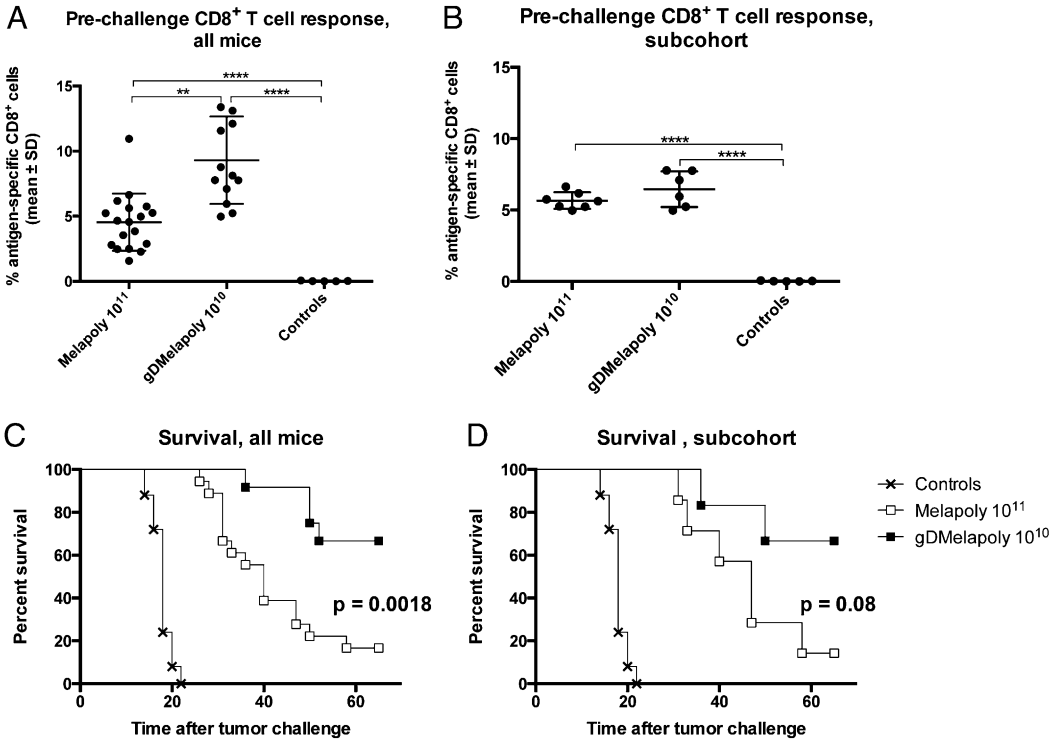

FIGURE 3. Vaccine efficacy in mice vaccinated before tumor cell challenge. Groups of C57BL/6 mice (n = 5-18) were vaccinated with 10^{11} vp AdC68-gD, 10^{11} vp AdC68-Melapoly, or 10^{10} vp AdC68-gDMelapoly vectors. Fourteen days later, PBMC samples were tested for $CD8^+$ T cell responses to all of the MAA epitopes present in the vaccine. (**A**) The sum of tumor Ag-specific $CD8^+$ T cell percentages for individual mice. *, Significant differences as detailed in legend to Fig. 1. Melapoly versus gDMelapoly: $p < 0.0001$, Melapoly versus naive: $p = 0.0014$, gDMelapoly versus naive: $p < 0.0001$. (**B**) The sum of tumor Ag-specific $CD8^+$ T cell percentages in the two subcohorts that showed comparable $CD8^+$ T cell responses. Subcohorts were selected by excluding animals with frequencies of MAA-specific $CD8^+$ T cells below the mean of the Melapoly group or above the mean of the gDMelapoly group. Melapoly versus gDMelapoly, $p = 0.1$, Melapoly versus naive: $p < 0.0001$, gDMelapoly versus naive: $p < 0.0001$. (**C**) Survival rates of the entire group, measured for 60 d. Melapoly versus naive: $p < 0.0001$, gD-Melapoly versus naive: $p < 0.0001$, Melapoly versus gDMelapoly: $p = 0.0018$. (**D**) Survival rates of the of the Melapoly subcohort in comparison with the gDMelapoly and the control group. Melapoly versus controls: $p < 0.0001$, gD-Melapoly versus controls: $p = 0.0003$, Melapoly versus gDMelapoly: $p = 0.08$. In (C) and (D), control animals are shown as X, AdC68-Melapoly-vaccinated mice are shown as open squares, AdC68-gDMelapoly-vaccinated mice are shown as closed squares.

9.3% for Melapoly and gD-Melapoly, 0.02% for control cells). The AdC68-gDMelapoly vector induced significantly higher $CD8^+$ T cell responses compared with the AdC68-Melapoly vector ($p < 0.0001$), and this was linked to enhanced survival rates upon tumor challenge ($p = 0.0018$ by Gehan–Breslow–Wilcoxon test; Fig. 3C). Specifically, >60% of AdC68gD-Melapoly–vaccinated mice as compared with <20% of AdC68-Melapoly–vaccinated mice remained tumor free. When we compared subgroups with similar frequencies of MAA-specific $CD8^+$ T cells by removing the low responders from the Melapoly group and the high responders from the gD-Melapoly group (mean frequencies of the Melapoly subcohort: 5.7% and the gD-Melapoly subcohort: 6.5% $p = 0.1$; Fig. 3B), survival rates of the two vaccine groups ceased to be significantly different ($p = 0.08$; Fig. 3D). This suggests that in the pretumor challenge model vaccine efficacy is significantly influenced by the magnitude of MAA-specific $CD8^+$ T cell responses.

In a posttumor challenge vaccination model, gD adjuvant efficacy is not solely linked to the magnitude of MAA-specific $CD8^+$ T cell responses

We further compared the efficacy of the two vectors in a post-challenge vaccination model. $B16Braf_{V600E}$ cells grow very rapidly in vivo; after tumor cell inoculation, most control mice require euthanasia within 14–18 d. AdC68-induced T cell responses on the other hand do not peak till 12–14 d after vaccination. Therefore, we chose a fairly short interval of 3 d between tumor cell inoculation and vaccination for our therapeutic vaccine studies. Accordingly, groups of mice (n = 5–10) were challenged with $B16Braf_{V600E}$ tumor cells on day 0 and vaccinated 3 d later with either 10^{11} vp of the AdC68-Melapoly vector ($n = 9$) or 3×10^9vp and 10^{10} vp of the AdC68-gDMelapoly vector ($n = 8$ and 10 for 3×10^9 and 10^{10} vp, repectively). A control group ($n = 28$) was vaccinated with 10^{11} vp of the AdC68-gD vector. $CD8^+$ T cell responses were measured 2 wk later from blood by ICS for production of IFN-γ, TNF-α, granzyme B, and perforin. In addition, we assessed $CD8^+$ T cell responses by staining with the $Trp\text{-}1_{455}$– and $Trp\text{-}2_{180}$–specific tetramers. MAA-specific $CD8^+$ T cell responses tested by ICS were significantly higher compared with background stains for both vaccine groups, and higher in gDMelapoly than Melapoly-vaccinated mice (means: Melapoly: 3.6%, gD-Melapoly: 5.2%, controls: 0.27%, adjusted p values are shown in the figure legend; Fig. 4Aa). The AdC68-gDMelapoly and Melapoly vector induced significantly higher frequencies of $Trp\text{-}1_{455}$ (means: Melapoly: 5.2%, gD-Melapoly: 6.3%, controls: 0.037%; Fig. 4Ba) and $Trp\text{-}2_{180}$ $tetramer^+CD8^+$ T cells (means: Melapoly: 0.19% and gD-Melapoly: 0.14% control cells: 0.042%; Fig. 4Ca) compared with controls. Both vaccines significantly delayed tumor growth and prolonged overall survival compared with control mice ($p < 0.0001$; Fig. 4Da). Comparing the two vaccine groups showed that AdC68-gDMelapoly–vaccinated mice survived significantly longer than AdC68-Melapoly–vaccinated mice ($p = 0.0039$; Fig. 4Ad).

Because MAA-specific $CD8^+$ T cell responses were higher in the AdC68-gDMelapoly group than in the Melapoly group, we selected eight mice from the AdC68-Melapoly vaccine group and

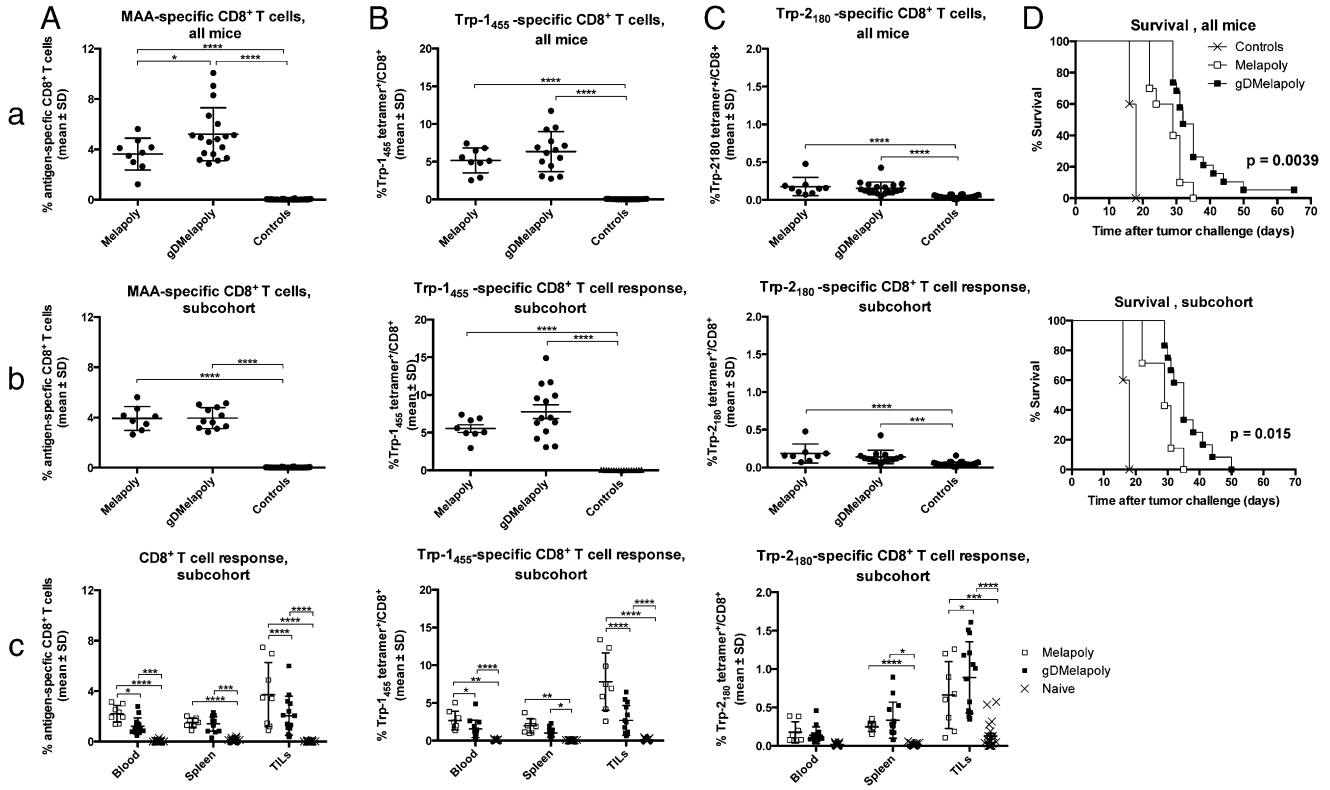

FIGURE 4. Vaccine efficacy in mice vaccinated after tumor cell challenge. Groups of C57BL/6 mice (n = 9–30) were challenged with B16Braf$_{V600E}$ cells given s.c. 3 d before vaccination with 10^{11} vp AdC68-gD, 10^{11} vp AdC68-Melapoly or 3×10^{9} and 10^{10} vp AdC68-gDMelapoly vector. Subcohorts were selected by excluding animals that had frequencies of MAA-specific CD8$^+$ T cells below the mean of the Melapoly group divided by the fold difference between the gDMelapoly over Melapoly group (1.34) or above the mean of the gDMelapoly group multiplied by the fold difference. (**a** and **b**) PBMCs were tested 12 d after vaccination. (**c**) Cells from blood, spleens, and tumors were tested at necropsy. (a**A**–a**D**) shows responses and survival rates of all mice, (bA–bD) and (cA–cC) show responses and survival rates of the subcohorts. *, Significant difference between two groups as described in legend to Fig. 1 with the following p values: (**A**a) both vaccine groups versus controls: $p < 0.0001$; Melapoly versus gDMelapoly: $p = 0.01$. (Ab) both vaccine groups versus to controls: $p < 0.0001$; Melapoly versus gDMelapoly: $p = 0.99$. (Ac) Blood: Melapoly versus controls: $p < 0.0001$, gDMelapoly versus controls: $p = 0.0003$, Melapoly versus gDMelapoly: $p = 0.011$, Spleen: Melapoly versus controls: $p = 0.0003$, gDMelapoly versus controls: $p < 0.0001$, Tumors: all comparisons: $p < 0.0001$. (**B**a) both vaccines versus controls $p < 0.0001$, Melapoly versus gDMelapoly $p = 0.28$. (Bb) both vaccine groups versus controls: $p < 0.0001$, Melapoly versus gDMelapoly: $p = 0.07$. (Bc) Blood: Melapoly versus controls: $p < 0.0001$, gDMelapoly versus controls: $p = 0.0029$, Melapoly versus gDMelapoly $p = 0.047$, Spleen: Melapoly versus controls: $p < 0.0001$, gDMelapoly versus controls: $p = 0.04$, Tumors: all comparisons: $p < 0.0001$. (**C**a) both vaccines versus controls: $p < 0.0001$. (Cb) Melapoly versus controls: $p < 0.0001$, gDMelapoly versus controls: 0.0002. (Cc) Spleen: Melapoly versus controls: $p = 0.02$, gDMelapoly versus controls: $p < 0.0001$, Tumors: both vaccine groups versus controls: $p < 0.0001$, Melapoly versus gDMelapoly, $p = 0.0187$.

14 mice from the AdC68-gDMelapoly vaccine group with comparable frequencies of total cytokine$^+$CD8$^+$ T cell responses (means, Melapoly: 3.9%, gDMelapoly: 4.0%; Fig. 4Ab), Trp-1$_{455}$ tetramer$^+$CD8$^+$ T cells (means, Melapoly: 3.0% and gDMelapoly: 3.1%; Fig. 4Bb) and Trp-2$_{180}$ tetramer$^+$CD8$^+$ T cell responses (means, Melapoly: 0.19% and gD-Melapoly 0.14%; Fig. 4Cb). Again, in the subcohorts, both vaccines significantly delayed tumor growth and prolonged survival compared with control mice ($p < 0.0001$). Although mice had been selected based on comparable frequencies of MAA-specific CD8$^+$ T cell responses, the AdC68-gDMelapoly–vaccinated subcohort showed significantly prolonged survival rates compared with the AdC68-Melapoly–vaccinated subcohort ($p = 0.015$; Fig. 4Db).

To assess whether vaccine-induced T cell responses differed in tissues, we analyzed MAA-specific CD8$^+$ T cell responses to all epitopes by ICS in the blood, spleens, and tumors at the time of necropsy when the size of tumor exceeded a surface area of ~100 mm^2. Interestingly, total cytokine$^+$CD8$^+$ T cell responses in the blood and tumors of AdC68-Melapoly–vaccinated mice were significantly higher than those of AdC68-gDMelapoly–vaccinated mice (mean frequencies: blood, spleens, tumors: Melapoly: 2.2, 1.5, and 3.7%; gD-Melapoly: 1.2, 1.4, and 2.1%; controls: 0.049, 0.12, and 0.027%; Fig. 4Ac, p values are shown in the figure legend). For Trp-1$_{455}$–specific CD8$^+$ T cell responses, both vaccines induced significant responses in the different compartments compared with naive cells. The AdC68-Melapoly group again showed significantly higher responses in tumors compared with mice immunized with AdC68-gDMelapoly (mean frequencies: blood, spleens, and tumors: Melapoly: 2.7, 2.0, and 7.8%; gD-Melapoly: 1.6, 1.0, and 2.7%; controls: 0.085, 0.043, and 0.14%; Fig. 4Bc; gating strategies Supplemental Fig. 3). Trp-2$_{180}$–specific responses were insignificant in blood but reached significance for both vaccine groups for cells from spleens and tumors compared with naive samples (mean frequencies: blood, spleens, and tumors: Melapoly: 0.18, 0.25, and 0.66%; gDMelapoly: 0.14, 0.33, and 0.89%; controls: 0.016, 0.02, and 0.13%; Fig. 4Bc). MAA-specific CD4$^+$ T cell responses were analyzed in parallel; they showed no differences before challenge but after challenge were higher in spleens of Melapoly-vaccinated mice (mean frequencies in spleens 1.5 and 0.59% for Melapoly and gD-Melapoly, respectively, p = 0.012; data not shown). Overall, these results indicated that in the postchallenge vaccine model better protection achieved with the gD adjuvanted vaccine could not solely be explained by induction of higher frequencies of MAA-specific CD8$^+$ T cells.

MAA-specific CD8$^+$ T cell phenotypes

Chronic exposure to Ag can lead to T cell exhaustion, which is characterized by progressive loss of T cell functions and eventual cell death (26, 27). To determine whether gD affected the differentiation pathways of T cells, we assessed the expression of several exhaustion markers (i.e., 2B4, LAG-3, and PD-1) on Trp-1_{455}- and Trp-2_{180}-specific CD8$^+$ T cells in spleens and tumors at the time of necropsy, using the two subcohorts with comparable CD8$^+$ T cell responses. Expression of exhaustion markers was also assessed on CD44$^-$CD8$^+$ (naive) T cells and CD44$^+$tet$^-$CD8$^+$ (memory) T cells. The latter population, negative for Trp-1_{455} and Trp-2_{180} tetramer–specific CD8$^+$ T cells, presumably contained CD8$^+$ T cells to other MAAs in the vaccine and to unrelated Ags encountered previously. Fig. 5A shows expression levels of the three exhaustion markers as mean fluorescence intensity (MFI) of the different dyes attached to the marker-specific Abs. Significant differences were found between CD44$^-$CD8$^+$ and CD44$^+$CD8$^+$ T cells in spleens and tumors only for 2B4 (Fig. 5A). Differences between CD44$^-$CD8$^+$ or CD44$^+$CD8$^+$ T cells and vaccine-induced tetramer$^+$CD8$^+$ T cells were seen for all markers with the exceptions of 2B4 on Trp-$1_{455}{}^+$CD8$^+$ cells from spleens and 2B4 and PD-1 on Trp-$2_{180}{}^+$CD8$^+$TILs. We also observed significant differences between the two vaccine subcohorts as well as between CD8$^+$ T cells to the two epitopes. In particular, 2B4 showed higher expression on Trp-2_{180}- than Trp-1_{455}-specific CD8$^+$ T cells induced by either vaccine in spleens (mean MFI Melapoly: Trp-1_{455} versus Trp-2_{180}: 158 versus 269, gDMelapoly: Trp-1_{455} versus Trp-2_{180}: 166 versus 284, adjusted p values are shown in the legend to Fig. 5A). In both vaccine groups LAG-3 expression in spleens and in tumors was higher on Trp-1_{455}– than Trp-2_{180}–specific CD8$^+$ T cells. In tumors, Trp-1_{455}–specific CD8$^+$ T cells showed significantly lower level of LAG-3 expression in AdC68-gDMelapoly–vaccinated animals compared with those from AdC68-Melapoly–vaccinated mice (mean MFI: spleen: Melapoly: Trp-1_{455} versus Trp-2_{180}: 436 versus 224, gDMelapoly: Trp-1_{455} versus Trp-2_{180}: 401 versus 313; tumors: Melapoly: Trp-1_{455} versus Trp-2_{180}: 875 versus 504, gDMelapoly: Trp-1_{455} versus Trp-2_{180}: 728 versus 609). In spleens, PD-1 was expressed at higher levels on Trp-2_{180}– than Trp-1_{455}–specific CD8$^+$ T cells, and this reached significance for those induced by AdC68gD-Melapoly. Within tumors again Trp-1_{455}–specific CD8$^+$ T cells that had been elicited by the AdC68-gDMelapoly vaccine showed lower PD-1 expression compared with those elicited by the AdC68-Melapoly vaccine. In both vaccine groups, Trp-1_{455}–specific CD8$^+$ T cells expressed higher levels of PD-1 compared with those specific for Trp-2_{180} (mean MFI: spleen: Melapoly: Trp-1_{455} versus Trp-2_{180}: 97 versus 126, gDMelapoly: Trp-1_{455} versus Trp-2_{180}: 89 versus 151; tumors: Melapoly: Trp-1_{455} versus Trp-2_{180}: 1190 versus 400, gDMelapoly: Trp-1_{455} versus Trp-2_{180}: 721 versus 297).

In addition, we determined the percentages of Trp-1_{455}– and Trp-2_{180}–specific CD8$^+$TILs that were positive for either of the exhaustion markers and compared the results with those on naive (CD44$^-$) or memory tetramer$^-$ CD8$^+$ T cells (Fig. 5B, Supplemental Fig. 4). Only very low percentages of CD44$^-$CD8$^+$ T cells expressed any of the three exhaustion markers (<2%). Percentages of marker$^+$CD44$^+$tet$^-$CD8$^+$ T cells were intermediate (2B4, 19 and 15%; LAG-3, 17 and 12%; and PD-1, 23 and 41% for Melapoly and gDMelapoly-vaccinated mice). Expression of individual markers was significantly higher on CD44$^+$CD8$^+$ cells than on naive cells. Percentages of Trp-1_{455}– or Trp-2_{180}–specific CD8$^+$ T cells positive for any of the three exhaustion markers were again significantly higher when compared with CD44$^-$CD8$^+$ or tetramer$^-$CD44$^+$CD8$^+$ cells. Comparing the two vaccine subcohorts or Trp-1_{455}– and Trp-2_{180}–specific CD8$^+$ T cells within each vaccine group showed no significant differences for percentages of 2B4$^+$ cells (means: Melapoly: Trp-1_{455} versus Trp-2_{180}: 52 versus 39%, gDMelapoly: Trp-1_{455} versus Trp-2_{180}: 44 versus 33%). LAG-3$^+$ cells were significantly more common within Trp-1_{455}–specific CD8$^+$ T cells in both vaccine groups (means: Melapoly: Trp-1_{455} versus Trp-2_{180}: 87 versus 48%, gDMelapoly: Trp-1_{455} versus Trp-2_{180}: 81 versus 58%) as were PD-1$^+$CD8$^+$ cells in Melapoly-vaccinated mice. Interestingly percentages of PD-1$^+$ Trp-1_{455}–specific CD8$^+$ cells were significantly lower in the AdC68gD-Melapoly group than in mice immunized with Melapoly (means: Melapoly: Trp-1_{455} versus Trp-2_{180}: 84 versus 67%, gDMelapoly: Trp-1_{455} versus Trp-2_{180}: 63 versus 57%).

Exhaustion leads to sequential expression of several markers (27). Accordingly, we further analyzed tumor-derived T cells for coexpression of PD-1, LAG-3, and 2B4 (Fig. 5B). Again we found that higher percentages of Trp-1_{455}– and Trp-2_{180}–specific CD8$^+$ T cells coexpressed two or three markers compared with CD44$^-$ CD8$^+$ or tetramer$^-$CD44$^+$CD8$^+$ cells. Trp-1_{455}–specific CD8$^+$ T cells had in general higher frequencies of PD-1$^+$LAG-3$^+$ and PD-1$^+$LAG-3$^+$2B4$^+$ cells compared with Trp-2_{180}–specific CD8$^+$ T cells. Trp-1_{455}–specific CD8$^+$ cells expressing two or three of the markers were present at significantly lower frequencies in gDMelapoly than Melapoly-immunized mice (means: Melapoly versus gDMelapoly: PD-1$^+$2B4$^+$: Trp-1_{455}: 47 versus 35%, Trp-2_{180}: 32 versus 24%; PD-1$^+$LAG-3$^+$: Trp-$1_{455:}$ 69 versus 53%, Trp-2_{180}: 29 versus 24%; PD-1$^+$2B4$^+$LAG-3$^+$: Trp-$1_{455:}$ 45 versus 34%, and Trp-2_{180}: 25 versus 20%).

Markers that are indicative for exhaustion are also upregulated upon activation. To ensure that AdC68-gDMelapoly–induced TILs showed better preservation of function as would be expected of less exhausted CD8$^+$ T cells, we compared the proportions of Trp-1 specific CD8$^+$ T cells that produced only IFN-γ or IFN-γ together with TNF-α between the two vaccine groups. For these comparisons cells were isolated from tumors at days 30–35 after vaccination. AdC68-gDMelapoly–induced Trp-1–specific CD8$^+$ T cells had significantly higher proportions of Trp-1–specific CD8$^+$ TILs that produced both cytokines compared with AdC68-Melapoly–induced TILs (mean AdC68-gDMelapoly: 0.47, AdC68-Melapoly: 0.3, $p = 0.04$ by two-tailed t test). To further ensure that Trp-1–specific TILs with increased expression of PD-1 or PD-1 and LAG-3 were indeed exhausted rather than recently activated, we tested PD-1$^+$ and PD-1$^-$ TILs for production of IFN-γ and TNF-α upon stimulation with the Trp-1_{455} peptide. As shown in Fig. 6A, slightly higher frequencies of Trp-1–specific CD8$^+$ T cells from blood produced IFN-γ together with TNF-α than IFN-γ only. In tumors this proportion shifted and ~70% of Trp-1–specific TILs produced only IFN-γ suggesting loss of function (mean frequencies of Trp-1–specific CD8$^+$ T cells: blood: IFN-γ$^+$TNF-α$^-$ versus IFN-γ$^+$TNF-α$^+$: 0.32 versus 0.57%; tumor: 1.85 versus 0.84%). Costains for PD-1 showed significantly higher PD-1expression on monofunctional Trp-1–specific CD8$^+$ TILs as compared with those that produced both cytokines (mean PD-1 MFI values: blood: IFN-γ$^+$TNF-α$^-$ versus IFN-γ$^+$TNF-α$^+$: 174 versus 143, .tumor: 1236 versus 774; Fig. 6B). An analysis for expression of T-bet, which controls transcription of effector molecules and inhibits expression of PD-1, showed that T-bet levels were low on naive circulating CD8$^+$ T cells and markedly increased on blood-derived Trp-1–specific CD8$^+$ T cells. Tumor-infiltrating Trp-1–specific CD8$^+$ T cells showed a marked reduction in T-bet expression (Fig. 6C), which corresponded to expression levels of exhaustion/activation markers (mean T-bet MFI values: CD44$^-$CD8$^+$ T cells: 6.2; Trp-1 specific CD8$^+$

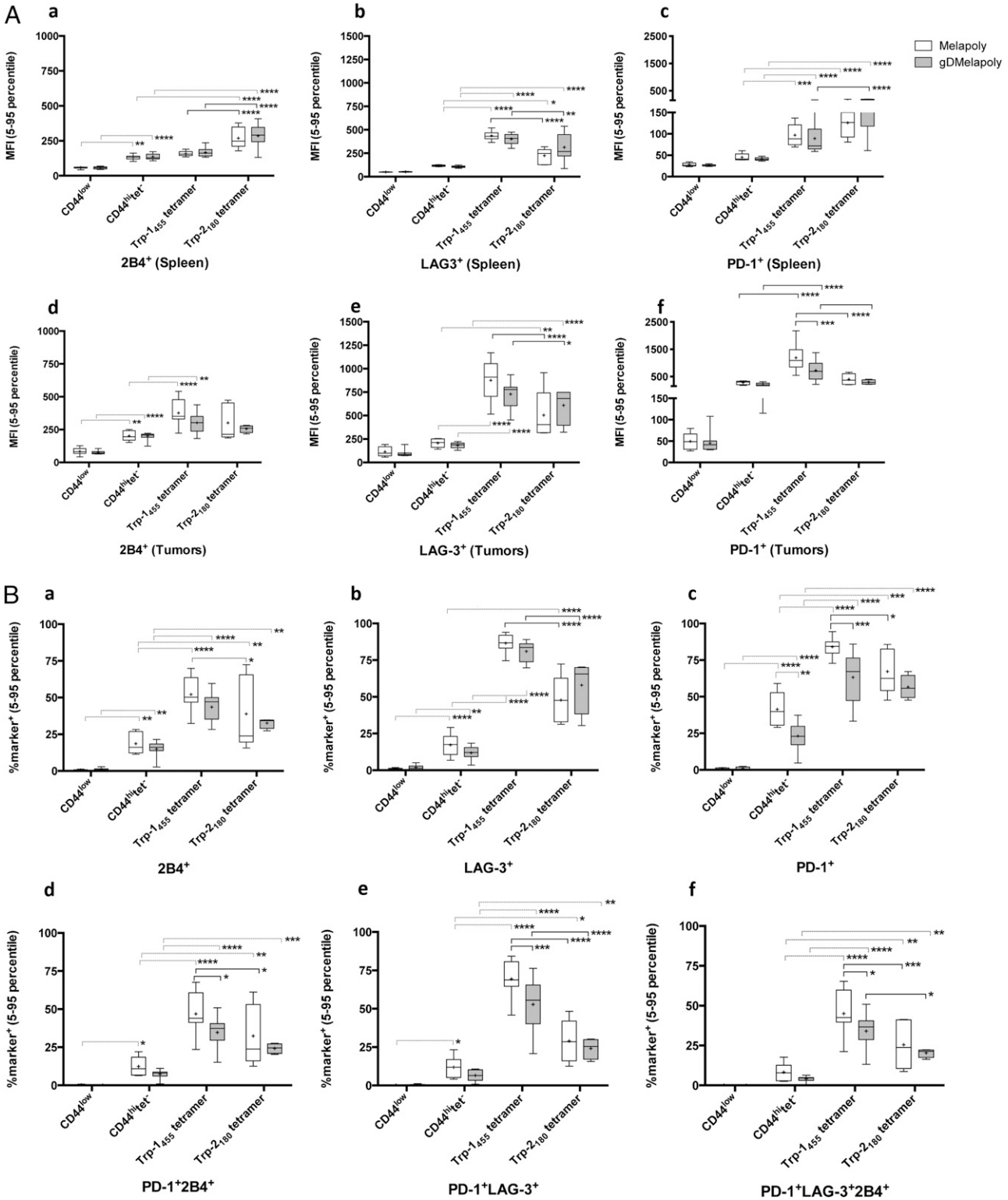

FIGURE 5. MAA-specific $CD8^+$ T cell phenotypes. Phenotypes of $CD8^+$ T cells isolated from spleens and tumors of the two subcohorts shown in Fig. 4 were tested for expression of 2B4, LAG-3, and PD-1. (**A**) MFI of 2B4 (**a**, **d**), LAG-3 (**b**, **e**), and PD-1 (**c**, **f**) fluorochrome-labeled Abs on $CD44^-CD8^+$, tetramer$^-$CD44$^+$CD8$^+$ and tetramer$^+$CD44$^+$CD8$^+$ T cells from spleens (a–c) and tumors (d, f). Open boxes show results for $CD8^+$ T cells from AdC68-Melapoly–vaccinated mice, gray boxes indicated $CD8^+$ T cells from AdC68-gDMelapoly vaccinated mice. *, Significant differences as detailed in legend to Fig. 1 between groups connected by lines (dashed lines for differences between control cells or between control cells and Ag-specific $CD8^+$ T cells, solid lines for differences between specific $CD8^+$ T cells). The following p values were obtained for Trp-1_{455} and Trp-2_{180} comparisons: (Aa) Trp-1_{455} versus Trp-2_{180}: Melapoly: $p < 0.0001$, gDMelapoly: $p < 0.0001$; (Ad) none; (Ab) Trp-1_{455} versus Trp-2_{180}: Melapoly: $p < 0.0001$, gDMelapoly: $p = 0.0056$; (Ae) Trp-1_{455} versus Trp-2_{180}: Melapoly: $p < 0.0001$; (Ac) Trp-1_{455} versus Trp-2_{180}: gDMelapoly: $p < 0.0001$; (Af) Trp-1_{455} versus Trp-2_{180}: Melapoly: $p < 0.0001$, gDMelapoly: $p = 0.028$, Melapoly versus gDMelapoly: Trp-1_{455}: $p = 0.0008$. (**B**) Percentages of tumor-derived naive $CD44^-CD8^+$, tetramer$^-$CD44$^+$CD8$^+$, and tetramer$^+$CD44$^+$CD8$^+$ T cells that were positive for a given marker or combinations of exhaustion markers. Cells from AdC68-Melapoly–vaccinated mice are shown as open boxes, and cells from AdC68-gDMelapoly vaccinated mice are shown as gray boxes. Whiskers show 5–95th percentile, lines show 50th percentile, + within boxes indicates means. *, Significant differences between groups as described in legends to Fig. 1. (B**a**) (*Figure legend continues*)

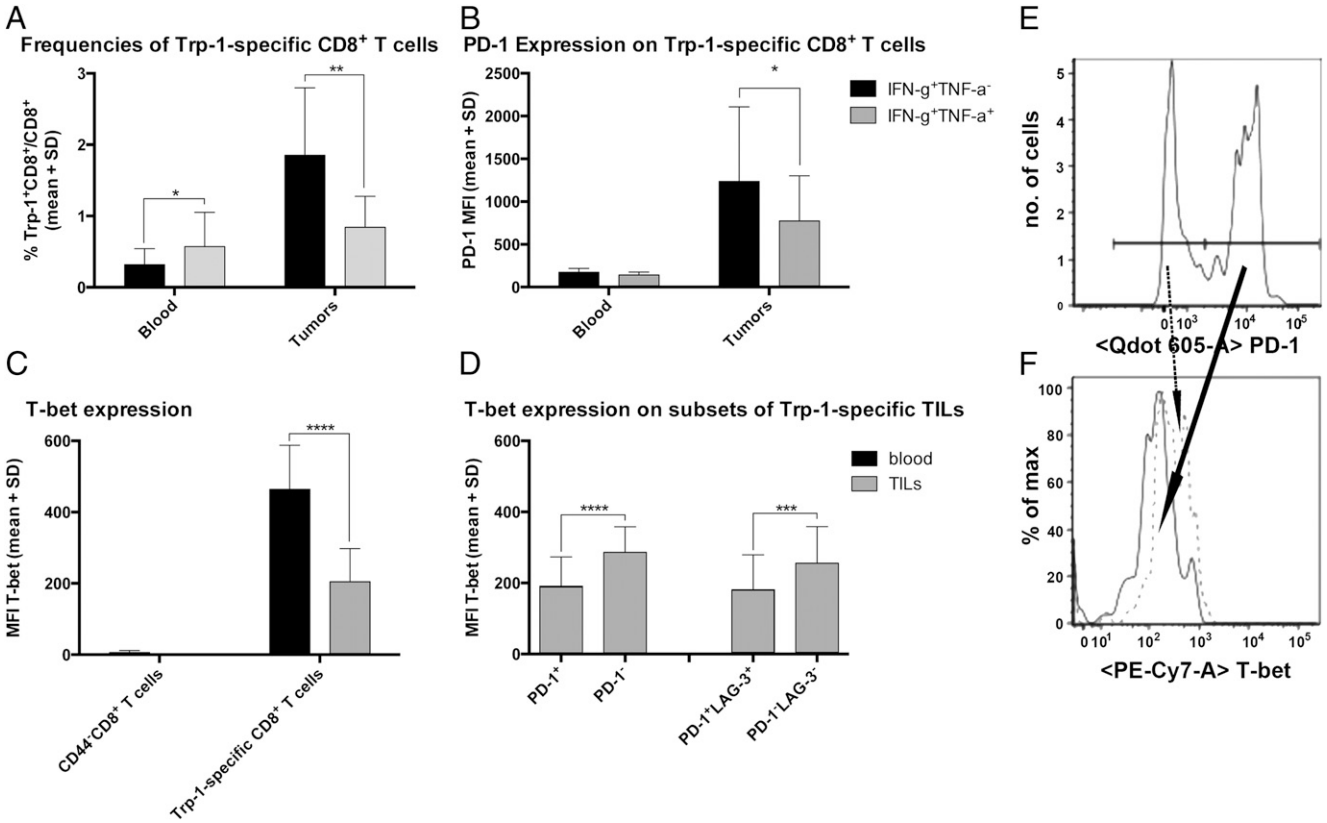

FIGURE 6. MAA-specific T cell functions in relation to phenotypes. Mice with 3-d-old B16Braf$_{V600E}$ tumors were vaccinated with 10^{10} vp AdC68-gDMelapoly. Lymphocytes from blood and tumors were isolated 4 wk later. (**A**) Frequencies of CD8$^+$ T cells producing IFN-γ only or IFN-γ together with TNF-α were determined by ICS. By *t* tests frequencies of Trp-1–specific IFN-γ$^+$TNF-α$^+$CD8$^+$ T cells were higher in blood than those of IFN-γ$^+$TNF-α$^-$ CD8$^+$ T cells ($p = 0.036$), whereas in TILs, frequencies of Trp-1-specific CD8$^+$ T cells producing only IFN-γ were significantly higher ($p = 0.0066$). (**B**) shows levels of PD-1 expression on Trp-1–specific CD8$^+$ T cells that produced only IFN-γ or IFN-γ together with TNF-α. Expression levels were comparable in blood-derived cells but significantly higher on TILs that were only positive for IFN-γ than on those that produced both cytokines ($p = 0.024$). (**C**) shows levels of T-bet expression on naive CD44$^-$CD8$^+$ lymphocytes from blood and on Trp-1–specific CD8$^+$ T cells from blood and tumors. Trp-1–specific CD8$^+$ T cells expressed significantly higher levels of T-bet as compared with naive CD8$^+$ T cells ($p < 0.0001$). T-bet expression was higher on blood than on tumor-derived Trp-1–specific CD8$^+$ T cells ($p < 0.0001$). (**D**) shows levels of T-bet expression on Trp-1–specific TILs separated into subgroups according to levels of PD-1 or PD-1 and LAG-3 expression. Levels of T-bet expression were significantly higher on PD-1$^-$ as compared with PD-1$^+$ cells ($p = 0.0001$) and on PD-1$^-$LAG-3$^-$ cells than on PD-1$^+$LAG-3$^+$ cells ($p = 0.0002$). (**E**) Gating scheme onto PD-1$^+$ and PD-1$^-$ cells following initial gating on live lymphoid cells, CD8$^+$ cells, CD44^{hi} cells, and Trp-1 tetramer$^+$ cells as shown in Supplemental Fig. 1. (**F**) Expression levels of T-bet on PD-1$^-$ (dashed line) and PD-1$^+$ Trp-1–specific CD8$^+$ T cells.

T cells blood versus TILs: 464.2 versus 204.6); Trp-1-specific CD8$^+$ TILs that expressed high levels of PD-1 or PD-1 and LAG-3 had reduced levels of T-bet as compared with those with low PD-1 or PD-1 and LAG-3 expression (Fig. 6D–F) (mean T-bet MFI values: PD-1$^+$ versus PD-1$^-$: 191.4 versus 286.2; PD-1$^+$LAG-3$^+$ versus PD-1$^-$LAG-3$^-$: 181.3 versus 256). Overall these results show that increased expression of PD-1 was associated with loss of polyfunctionality and downregulation of T-bet, confirming that MAA-specific CD8$^+$ T cells induced by the vaccines were differentiation toward exhaustion within the TME.

Taken together, these results demonstrate complex patterns of up-regulation of exhaustion markers during tumor progression that were affected by the vaccines, the TcR specificity as well as the anatomic sites from which T cell had been isolated. Within tumors, MAA-specific CD8$^+$ T cells induced by the AdC68-gDMelapoly vector were less exhausted compared with those induced by the AdC68-Melapoly vector, fewer cells expressed exhaustion markers, and they were able to delay tumor progression for longer periods of time. In addition, tumor-infiltrating CD8$^+$ T cells specific to the dominant Trp-1$_{455}$ epitopes showed more evidence of exhaustion compared with those specific to the subdominant Trp-2$_{180}$ epitope.

Discussion

T cell activation is finely tuned upon binding of the TcR to its cognate Ag-MHC class I molecule complex through additional interactions with costimulatory and coinhibitory receptors (28, 29). Coinhibitory receptors include CTLA-4, PD-1, BTLA, and others. BTLA, unlike PD-1 and CTLA-4, is expressed on both naive and activated T cells (30) and thereby presumably regulates T cell activation at several stages. PD-1 and CTLA-4 inhibit downstream signals transmitted upon TcR ligation such as induction of the

Trp-1$_{455}$ versus Trp-2$_{180}$: Melapoly: $p = 0.031$. (B**d**) Melapoly versus gDMelapoly: Trp-1$_{455}$: $p = 0.035$; Trp-1$_{455}$ versus Trp-2$_{180}$: Melapoly: 0.019. (B**b**): Trp-1$_{455}$ versus Trp-2$_{180}$: Melapoly: $p < 0.0001$, gDMelapoly: $p < 0.0001$. (B**e**) Melapoly versus gDMelapoly: Trp-1$_{455}$: $p = 0.0036$; Trp-1$_{455}$ to Trp-2$_{180}$: Melapoly: $p < 0.0001$, gDMelapoly: $p < 0.0001$. (B**c**) Melapoly versus gDMelapoly: Trp-1$_{455}$: $p = 0.0006$, Trp-1$_{455}$ versus Trp-2$_{180}$: Melapoly $p = 0.016$. (B**f**) Melapoly versus gDMelapoly: Trp-1$_{455}$: $p = 0.039$; Trp-1$_{455}$ versus Trp-2$_{180}$: Melapoly: $p = 0.0004$, gDMelapoly: $p = 0.021$.

protein kinase B pathway, albeit through distinct pathways (31, 32). Protein kinase B pathway in turn regulates cell survival as well as glucose metabolism and is therefore crucial for successful activation and expansion of T cells (33). The exact signaling pathway downstream of BTLA remains unknown. Similar to PD-1 and CTLA-4, the cytoplasmic domain of BTLA contains immune receptor tyrosine–based inhibitory motifs (34) that may dampen TcR signaling.

Although modulators of HVEM signaling have not yet been tested in humans, the TNFRSF14 locus, which encodes HVEM, has been linked to increased risks for ulcerative colitis (35), systemic lupus erythomatodus (36), and rheumatoid arthritis (37), stressing the importance of this regulatory pathway. Similarly, genetic deletions of BTLA or HVEM cause exacerbated inflammatory reactions (38) and accelerated rejection of partially mismatched transplants in mice (39).

It has been shown that HVEM is expressed on tumor cells such as B cell lymphomas (40) or metastatic melanomas (41). BTLA on the other hand is highly expressed on melanoma-specific $CD8^+$ T cells and it has been argued that the impaired proliferative capacity of MAA-specific T cell in melanoma patients is linked to immunoinhibitory signals from $HVEM^+$ tumor cells (41). In another study, NY-ESA-1–specific $CD8^+$ T cells from end-stage melanoma patients were shown to express elevated levels of PD-1 and BTLA (42). T cells were defective in their ability to proliferate or secret factors in response to antigenic stimulation, which could in part be restored by blocking PD-1 and/or BTLA signaling. This suggests that inhibitors of BTLA should be explored as additives to active immunotherapy of melanoma.

As we showed previously, blockade of the BTLA-HVEM pathway through HSV-1 gD during Ag-driven T cell stimulation numerically augments $CD8^+$ T cell responses (17, 18). This was confirmed in the current study using vaccines expressing multiple epitopes derived from MAAs. In a prophylactic melanoma model, the superior protection achieved upon gD-mediated blockade of the HVEM pathways at the time of T cell induction was correlated with the magnitude of MAA-specific $CD8^+$ T cell responses. Using different doses of the two vaccines (i.e., AdC68-Melapoly and AdC68-gDMelapoly) mice that developed approximately equal frequencies of MAA-specific T cells showed comparable levels of protection against tumor protection. In contrast, in mice that were inoculated first with melanoma cells and then vaccinated with either of the two vectors, the magnitude of the vaccine-induced MAA-specific $CD8^+$ T cell response was not the sole factor that determined vaccine efficacy; in mice with approximately comparable frequencies of MAA-specific $CD8^+$ T cells following vaccination with the AdC68-Melapoly or AdC68-gDMelapoly vectors, those that received the latter survived significantly longer. Cytokine profiles of Ag-specific $CD8^+$ T cells were largely comparable between the two vaccine groups before and after challenge with responses being dominated by $CD8^+$ T cells producing IFN-γ alone or in combination with TNF-α (data not shown) as is typical for T cells induced by Ad vectors.

Paradoxically, at the time of necropsy AdC68-Melapoly–vaccinated animals had significantly higher frequencies of MAA-specific $CD8^+$ T cells in some tissues compared with those vaccinated with AdC68-gDMelapoly. This again confirms that protection did not solely correlate with frequencies of vaccine-induced T cells. Further analysis of MAA-specific $CD8^+$ T cells for expression of activation/exhaustion markers showed that within tumors lower frequencies of AdC68-gDMelapoly–induced $CD8^+$ T cells expressed LAG-3, PD-1, and PD-1 together with LAG-3 or 2B4 or all three markers as compared with AdC68-Melapoly–induced $CD8^+$ T cells. These markers are not only indicative for exhaustion but they are also increased upon recent $CD8^+$ T cells activation. Ags derived from the tumor may have provided further activation signals to the MAA-specific $CD8^+$ T cells, which then contributed to their elevated levels on tumor-infiltrating MAA-specific $CD8^+$ T cells. Nevertheless, as these activation signals should have been provided in both vaccine cohorts, we assume that the differences in expression levels on tumor-infiltrating MAA-specific $CD8^+$ T cells in Melapoly and gDMelapoly-vaccinated reflected differences in their stage of exhaustion. This was further confirmed by loss of polyfunctionality and T-bet expression on cells with increased expression of immunoinhibitory markers. In turn, our finding suggests that the relative resistance to tumor-driven exhaustion of MAA-specific $CD8^+$ T cells generated in presence of gD resulted in prolonged control of tumor progression.

T cell exhaustion, a consequence of continued Ag-driven-stimulation of T cells, was initially described in chronic viral diseases such as those caused by lymphocytic choriomeningitis virus infection of mice (26) or HIV (43) or hepatitis C virus infection (44) of humans and subsequently in cancer patients (45, 46). Differentiation toward exhaustion is initially characterized by increased expression of PD-1 on the T cell surface, which over time is joined by other coinhibitors (47). Expression of PD-1 is regulated by TcR ligation (48) and at the transcriptional level by NFAT1c (49). T cells with high-affinity TcRs appear to be more sensitive to Ag-driven exhaustion compared with those with lower affinity TcRs (50). This is supported by our finding that within tumors $CD8^+$ T cells specific to the subdominant Trp-2_{180} epitope appeared less exhausted; vaccine-induced Trp-2_{180}–specific $CD8^+$T cells expressed lower levels of PD-1 or LAG-3 as compared with $CD8^+$ T cells specific to the more dominant Trp-1_{455} epitope. The same pattern was seen for MAA-specific $CD8^+$ T cells that were double or triple positive for PD-1, 2B4, and/or LAG-3. Notwithstanding, it should be pointed out that the finding that higher TcR affinity promotes exhaustion remains debatable, although it is compatible with the highly reproducible finding that exhaustion is primarily driven by continued TcR ligation (51). Other pathways that prevent Ag-driven exhaustion of $CD8^+$ T cells used by the gD-adjuvanted vaccine may have contributed the results, but cannot be explored without additional knowledge of the BTLA/CD160 signaling pathways.

Active cancer immunotherapy with traditional vaccines that boost tumor-specific T cell responses has performed poorly in patients with advanced cancer. Additional strategies that block the immunoinhibitory pathways may improve the efficacy of cancer vaccines. In this study, we show that adjuvanting a tumor vaccine with HSV-1 gD could induce tumor Ag-specific $CD8^+$ T cells with increased resistance to exhaustion. This approach, unlike other reagents that block immunological checkpoints such as Abs to PD-1 or CTLA-4, selectively affects tumor Ag-specific T cells and presumably will not globally perturb the exquisitely fine-tuned balance of the immune system.

Acknowledgments

We thank the National Institutes of Health Tetramer Core Facility (Emory University Vaccine Center, Atlanta, GA) for providing the tetramers, Dr. M. Herlyn (Wistar Institute Melanoma Research Center, Philadelphia, PA) for providing $B16Braf_{V600E}$ cell line, Dr. X.Y. Zhou for help with molecular cloning, Dr. Z.Q. Xiang and Y. Li for purifying the viral vectors, and C. Cole for assisting in the preparation of the manuscript.

Disclosures

The authors have no financial conflicts of interest.

References

1. Mittendorf, E. A., and P. Sharma. 2010. Mechanisms of T-cell inhibition: implications for cancer immunotherapy. *Expert Rev. Vaccines* 9: 89–105.
2. Finn, O. J. 2003. Cancer vaccines: between the idea and the reality. *Nat. Rev. Immunol.* 3: 630–641.

3. Haile, S. T., J. J. Bosch, N. I. Agu, A. M. Zeender, P. Somasundaram, M. K. Srivastava, S. Britting, J. B. Wolf, B. R. Ksander, and S. Ostrand-Rosenberg. 2011. Tumor cell programmed death ligand 1-mediated T cell suppression is overcome by coexpression of CD80. *J. Immunol.* 186: 6822–6829.
4. Jacobs, J. F., S. Nierkens, C. G. Figdor, I. J. de Vries, and G. J. Adema. 2012. Regulatory T cells in melanoma: the final hurdle towards effective immunotherapy? *Lancet Oncol.* 13: e32–e42.
5. Umansky, V., and A. Sevko. 2012. Melanoma-induced immunosuppression and its neutralization. *Semin. Cancer Biol.* 22: 319–326.
6. Izawa, S., K. Mimura, M. Watanabe, T. Maruyama, Y. Kawaguchi, H. Fujii, and K. Kono. 2013. Increased prevalence of tumor-infiltrating regulatory T cells is closely related to their lower sensitivity to H2O2-induced apoptosis in gastric and esophageal cancer. *Cancer Immunol. Immunother.* 62: 161–170.
7. Lipson, E. J. 2013. Re-orienting the immune system: Durable tumor regression and successful re-induction therapy using anti-PD1 antibodies. *OncoImmunology* 2: e23661.
8. Pardoll, D. M. 2012. The blockade of immune checkpoints in cancer immunotherapy. *Nat. Rev. Cancer* 12: 252-264.
9. Callahan, M. K., M. A. Postow, and J. D. Wolchok. 2013. Immunomodulatory therapy for melanoma: ipilimumab and beyond. *Clin. Dermatol.* 31: 191–199.
10. Duraiswamy, J., K. M. Kaluza, G. J. Freeman, and G. Coukos. 2013. Dual blockade of PD-1 and CTLA-4 combined with tumor vaccine effectively restores T-cell rejection function in tumors. *Cancer Res.* 73: 3591–3603.
11. Intlekofer, A. M., and C. B. Thompson. 2013. At the bench: preclinical rationale for CTLA-4 and PD-1 blockade as cancer immunotherapy. *J. Leukoc. Biol.* 94: 25–39.
12. Whitbeck, J. C., C. Peng, H. Lou, R. Xu, S. H. Willis, M. Ponce de Leon, T. Peng, A. V. Nicola, R. I. Montgomery, M. S. Warner, et al. 1997. Glycoprotein D of herpes simplex virus (HSV) binds directly to HVEM, a member of the tumor necrosis factor receptor superfamily and a mediator of HSV entry. *J. Virol.* 71: 6083–6093.
13. Steinberg, M. W., T. C. Cheung, and C. F. Ware. 2011. The signaling networks of the herpesvirus entry mediator (TNFRSF14) in immune regulation. *Immunol. Rev.* 244: 169–187.
14. Cai, G., and G. J. Freeman. 2009. The CD160, BTLA, LIGHT/HVEM pathway: a bidirectional switch regulating T-cell activation. *Immunol. Rev.* 229: 244–258.
15. Stiles, K. M., J. C. Whitbeck, H. Lou, G. H. Cohen, R. J. Eisenberg, and C. Krummenacher. 2010. Herpes simplex virus glycoprotein D interferes with binding of herpesvirus entry mediator to its ligands through downregulation and direct competition. *J. Virol.* 84: 11646–11660.
16. Lasaro, M. O., N. Tatsis, S. E. Hensley, J. C. Whitbeck, S.-W. Lin, J. J. Rux, E. J. Wherry, G. H. Cohen, R. J. Eisenberg, and H. C. Ertl. 2008. Targeting of antigen to the herpesvirus entry mediator augments primary adaptive immune responses. *Nat. Med.* 14: 205–212.
17. DiMenna, L., B. Latimer, E. Parzych, L. H. Haut, K. Töpfer, S. Abdulla, H. Yu, B. Manson, W. Giles-Davis, D. Zhou, et al. 2010. Augmentation of primary influenza A virus-specific $CD8^+$ T cell responses in aged mice through blockade of an immunoinhibitory pathway. *J. Immunol.* 184: 5475–5484.
18. Lasaro, M. O., M. Sazanovich, W. Giles-Davis, P. Mrass, R. M. Bunte, D. A. Sewell, S. F. Hussain, Y.-X. Fu, W. Weninger, Y. Paterson, and H. C. Ertl. 2011. Active immunotherapy combined with blockade of a coinhibitory pathway achieves regression of large tumor masses in cancer-prone mice. *Mol. Ther.* 19: 1727–1736.
19. Bacik, I., J. H. Cox, R. Anderson, J. W. Yewdell, and J. R. Bennink. 1994. TAP (transporter associated with antigen processing)-independent presentation of endogenously synthesized peptides is enhanced by endoplasmic reticulum insertion sequences located at the amino- but not carboxyl-terminus of the peptide. *J. Immunol.* 152: 381–387.
20. Kianizad, K., L. A. Marshall, N. Grinshtein, D. Bernard, R. Margl, S. Cheng, F. Beermann, Y. Wan, and J. Bramson. 2007. Elevated frequencies of self-reactive $CD8^+$ T cells following immunization with a xenoantigen are due to the presence of a heteroclitic $CD4^+$ T-cell helper epitope. *Cancer Res.* 67: 6459–6467.
21. Alexander, J., J. Sidney, S. Southwood, J. Ruppert, C. Oseroff, A. Maewal, K. Snoke, H. M. Serra, R. T. Kubo, A. Sette, et al. 1994. Development of high potency universal DR-restricted helper epitopes by modification of high affinity DR-blocking peptides. *Immunity* 1: 751–761.
22. Guevara-Patiño, J. A., M. E. Engelhorn, M. J. Turk, C. Liu, F. Duan, G. Rizzuto, A. D. Cohen, T. Merghoub, J. D. Wolchok, and A. N. Houghton. 2006. Optimization of a self antigen for presentation of multiple epitopes in cancer immunity. *J. Clin. Invest.* 116: 1382–1390.
23. Bergmann, C. C., Q. Yao, C. K. Ho, and S. L. Buckwold. 1996. Flanking residues alter antigenicity and immunogenicity of multi-unit CTL epitopes. *J. Immunol.* 157: 3242–3249.
24. Del Val, M., H.-J. Schlicht, T. Ruppert, M. J. Reddehase, and U. H. Koszinowski. 1991. Efficient processing of an antigenic sequence for presentation by MHC class I molecules depends on its neighboring residues in the protein. *Cell* 66: 1145–1153.
25. Zhou, D., X. Zhou, A. Bian, H. Li, H. Chen, J. C. Small, Y. Li, W. Giles-Davis, Z. Xiang, and H. C. J. Ertl. 2010. An efficient method of directly cloning chimpanzee adenovirus as a vaccine vector. *Nat. Protoc.* 5: 1775–1785.
26. Wherry, E. J., J. N. Blattman, K. Murali-Krishna, R. van der Most, and R. Ahmed. 2003. Viral persistence alters CD8 T-cell immunodominance and tissue distribution and results in distinct stages of functional impairment. *J. Virol.* 77: 4911–4927.
27. Wherry, E. J. 2011. T cell exhaustion. *Nat. Immunol.* 12: 492–499.
28. Sharpe, A. H. 2009. Mechanisms of costimulation. *Immunol. Rev.* 229: 5–11.
29. de Vries, I. J. M. 2013. The nature of activatory and tolerogenic dendritic cell-derived signal II. *Front. Immunol.* 4: 53.
30. Han, P., O. D. Goularte, K. Rufner, B. Wilkinson, and J. Kaye. 2004. An inhibitory Ig superfamily protein expressed by lymphocytes and APCs is also an early marker of thymocyte positive selection. *J. Immunol.* 172: 5931–5939.
31. Riley, J. L. 2009. PD-1 signaling in primary T cells. *Immunol. Rev.* 229: 114–125.
32. Parry, R. V., J. M. Chemnitz, K. A. Frauwirth, A. R. Lanfranco, I. Braunstein, S. V. Kobayashi, P. S. Linsley, C. B. Thompson, and J. L. Riley. 2005. CTLA-4 and PD-1 receptors inhibit T-cell activation by distinct mechanisms. *Mol. Cell. Biol.* 25: 9543–9553.
33. Hemmings, B. A., and D. F. Restuccia. 2012. PI3K-PKB/Akt pathway. *Cold Spring Harb. Perspect. Biol.* 4: a011189–a011189.
34. Gavrieli, M., N. Watanabe, S. K. Loftin, T. L. Murphy, and K. M. Murphy. 2003. Characterization of phosphotyrosine binding motifs in the cytoplasmic domain of B and T lymphocyte attenuator required for association with protein tyrosine phosphatases SHP-1 and SHP-2. *Biochem. Biophys. Res. Commun.* 312: 1236–1243.
35. Ananthakrishnan, A. N., E. C. Oxford, D. D. Nguyen, J. Sauk, V. Yajnik, and R. J. Xavier. 2013. Genetic risk factors for *Clostridium difficile* infection in ulcerative colitis. *Aliment Pharmacol. Ther.* 38: 522-530.
36. Chadha, S., K. Miller, L. Farwell, S. Sacks, M. J. Daly, J. D. Rioux, and T. J. Vyse. 2006. Haplotype analysis of tumour necrosis factor receptor genes in 1p36: no evidence for association with systemic lupus erythematosus. *Eur. J. Hum. Genet.* 14: 69–78.
37. Jung, H. W., S. J. La, J. Y. Kim, S. K. Heo, J. Y. Kim, S. Wang, K. K. Kim, K. M. Lee, H. R. Cho, H. W. Lee, et al. 2003. High levels of soluble herpes virus entry mediator in sera of patients with allergic and autoimmune diseases. *Exp. Mol. Med.* 35: 501–508.
38. Steinberg, M. W., O. Turovskaya, R. B. Shaikh, G. Kim, D. F. McCole, K. Pfeffer, K. M. Murphy, C. F. Ware, and M. Kronenberg. 2008. A crucial role for HVEM and BTLA in preventing intestinal inflammation. *J. Exp. Med.* 205: 1463–1476.
39. del Rio, M.-L., J. Kurtz, C. Perez-Martinez, A. Ghosh, J. A. Perez-Simon, and J.-I. Rodriguez-Barbosa. 2011. B- and T-lymphocyte attenuator targeting protects against the acute phase of graft versus host reaction by inhibiting donor anti-host cytotoxicity. *Transplantation* 92: 1085–1093.
40. Costello, R. T., F. Mallet, B. Barbarat, J.-M. Schiano De Colella, D. Sainty, R. W. Sweet, A. Truneh, and D. Olive. 2003. Stimulation of non-Hodgkin's lymphoma via HVEM: an alternate and safe way to increase Fas-induced apoptosis and improve tumor immunogenicity. *Leukemia* 17: 2500–2507.
41. Derré, L., J.-P. Rivals, C. Jandus, S. Pastor, D. Rimoldi, P. Romero, O. Michielin, D. Olive, and D. E. Speiser. 2010. BTLA mediates inhibition of human tumor-specific $CD8^+$ T cells that can be partially reversed by vaccination. *J. Clin. Invest.* 120: 157–167.
42. Fourcade, J., Z. Sun, O. Pagliano, P. Guillaume, I. F. Luescher, C. Sander, J. M. Kirkwood, D. Olive, V. Kuchroo, and H. M. Zarour. 2012. $CD8^+$ T cells specific for tumor antigens can be rendered dysfunctional by the tumor microenvironment through upregulation of the inhibitory receptors BTLA and PD-1. *Cancer Res.* 72: 887–896.
43. Kaufmann, D. E., and B. D. Walker. 2008. Programmed death-1 as a factor in immune exhaustion and activation in HIV infection. *Curr. Opin. HIV AIDS* 3: 362–367.
44. Dustin, L. B., and C. M. Rice. 2007. Flying under the radar: the immunobiology of hepatitis C. *Annu. Rev. Immunol.* 25: 71–99.
45. Baitsch, L., P. Baumgaertner, E. Devêvre, S. K. Raghav, A. Legat, L. Barba, S. Wieckowski, H. Bouzourene, B. Deplancke, P. Romero, et al. 2011. Exhaustion of tumor-specific $CD8^+$ T cells in metastases from melanoma patients. *J. Clin. Invest.* 121: 2350–2360.
46. Kim, P. S., and R. Ahmed. 2010. Features of responding T cells in cancer and chronic infection. *Curr. Opin. Immunol.* 22: 223–230.
47. Blackburn, S. D., H. Shin, W. N. Haining, T. Zou, C. J. Workman, A. Polley, M. R. Betts, G. J. Freeman, D. A. A. Vignali, and E. J. Wherry. 2009. Coregulation of $CD8^+$ T cell exhaustion by multiple inhibitory receptors during chronic viral infection. *Nat. Immunol.* 10: 29–37.
48. Wherry, E. J., S.-J. Ha, S. M. Kaech, W. N. Haining, S. Sarkar, V. Kalia, S. Subramaniam, J. N. Blattman, D. L. Barber, and R. Ahmed. 2007. Molecular signature of $CD8^+$ T cell exhaustion during chronic viral infection. *Immunity* 27: 670–684.
49. Oestreich, K. J., H. Yoon, R. Ahmed, and J. M. Boss. 2008. NFATc1 regulates PD-1 expression upon T cell activation. *J. Immunol.* 181: 4832–4839.
50. Hebeisen, M., L. Baitsch, D. Presotto, P. Baumgaertner, P. Romero, O. Michielin, D. E. Speiser, and N. Rufer. 2013. SHP-1 phosphatase activity counteracts increased T cell receptor affinity. *J. Clin. Invest.* 123: 1044–1056.
51. Bos, R., K. L. Marquardt, J. Cheung, and L. A. Sherman. 2012. Functional differences between low- and high-affinity $CD8^+$ T cells in the tumor environment. *OncoImmunology* 1: 1239–1247.